A Compact Disc Player and Repetitive Control

Richard C.H. Lee
Trinity Hall College
University of Cambridge
Supervisor: Dr. M.C. Smith

May 18, 1995

Contents

List of Figures

Notations

R_{error}	radial position error index.
F_{error}	focus position error index.
CA	sum signal of four photo-diodes.
RE	unbiased radial error.
FE	unbiased focus error.
j	complex square root of -1.
$\mathbb{R}_+$	the set of all non-negative real numbers.
$\mathbb{Z}_+$	the set of all non-negative integers.
$\mathcal{L}(\mathbb{R}_+, \mathbb{R}^p)$, $\ell(\mathbb{Z}_+, \mathbb{R}^p)$	function spaces.
$\mathcal{L}^2(\mathbb{R}_+, \mathbb{R}^p)$, $\ell^2(\mathbb{Z}_+, \mathbb{R}^p)$	Hilbert spaces.
$\mathcal{W}_T$, Ω_m	periodic signals with finite power.
P, G	continuous-time systems.
Ψ, Φ, Φ_L	discrete-time systems.
K_c, K_d	controllers.
w, z	continuous-time signals.
ω, ψ, ζ	discrete-time signals.
$\mathscr{L}$	Laplace transform.
$\hat{}$	Laplace transform, λ-transform.
$\tilde{}$	discrete Fourier transform.
$'$	transpose.
*	conjugate transpose.
$\mathcal{F}_l(\cdot,\cdot)$	lower linear fractional transformation.
$\mathcal{S}(\cdot,\cdot)$	star product.
$\overline{\sigma}$	maximum singular value.
λ_k	$e^{j\frac{2\pi}{T}k}$, $k \in \mathbb{Z}_+$.

Chapter 1

Introduction

Compact Disc (CD) system has been widely used in recently years. CD is advantageous over classical play records by its higher quality, smaller size, larger memory and reasonable price. Data in a CD are recorded digitally as a form of an engraved spiral track (in the order of micrometers) on a reflective metal disc. A CD player is an optical decoding device that reproduces high quality output (audio) signals from a CD. A laser beam of suitable wavelength, instead of a classical reproduction needle, is chosen as a data pick-up tool. As a result, the laser spot should shine on the CD with high demanding accuracy. Two degrees of freedom of the laser spot, namely Radial Movement and Focus Movement, have to be precisely controlled so as to minimize the effects of various sorts of disturbances. A CD is rotated when optical data is taken by the Optical Read Out Unit. Owing to this periodic nature, disturbances to the two movements are periodic. This motivates the need of Repetitive Control.

Repetitive Control deals with input signals which are periodic with known period. The main goal is to minimize the "size" of all output signals over a certain class of periodic inputs so that the whole system is internally stable. In this report, we only tackle with Finite Dimensional Linear Time Invariant (FDLTI) systems. There are two approaches to repetitive control of FDLTI continuous-time systems: analog controller design and sampled-data digital controller design. Applying this theory to the CD player situation, the input signals will be disturbances whereas the output signals will be the errors of the laser spot with respect to the radial movement and the focus movement.

In this report, detailed explanations of a CD player's mechanisms and control issues of radial movement and focus movement will be given in Chapter 2. Chapter 3 presents a complete theory of repetitive control in the sampled-data digital controller design. For the analog control design, some achievements and further potential developments are presented.

Chapter 2

Control Issues in a Compact Disc Player

2.1 Introduction

Compact Disc (CD) system was first introduced in the 1980's. Information in CD is stored digitally. CD system is advantageous over play records by its higher accuracy, higher density, lower prices, improved operability and multi-functionality [15]. Nowadays, we adopt this new technology in daily lives such as CD-ROM (large storage volume), audio CD and visual CD (high quality and high density). Throughout this chapter, we will concentrate on audio CD, as an illustration, and on the role of control theory playing in this area. The structure of a CD player and the control theory employed in its Radial Control Unit and Focus Control Unit will be elaborated. All the practical aspects and the data in this chapter will be based on the Philips CD930 model [6].

2.2 Compact Disc Mechanism

A compact disc is a circular transparent plastic (refractive index 1.55 ± 0.1) disc of diameter $120mm$ and thickness $1.2 \pm 0.1mm$. On the annulus with inner radius $23mm$ and outer radius $58mm$, there is a thin reflective metal film (mainly aluminium) coated as the recorded program area. Information is stored digitally on this metal film. On top of the disc, there is a hard protective layer covered the whole program area. Information is coded digitally as a spiral track of pits with depth $0.1\mu m$. Distance between two tracks is $1.6 \pm 0.1\mu m$ (about 625 tracks in $1mm$) and width of the track is $0.4\mu m$. Information signals are decoded by a reflected laser beam focused from the side

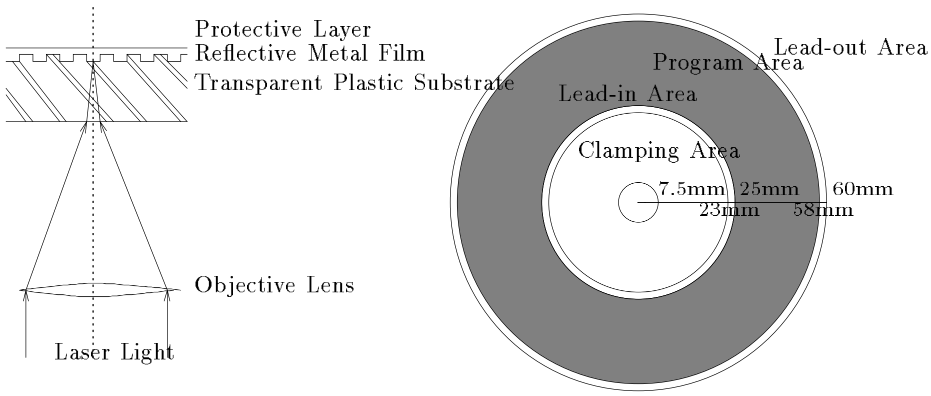

Figure 2.1: A typical Compact Disc

of the transparent layer (Figure 2.1). Why compact disc? Apart from its small size and its large capacity (playing time is over 60 minutes), signals are more resistant to dirt and scratches as the information is stored *inside* the disc. More importantly, recorded digital signals having sampling frequency $44.1kHz$ and quantization of 16 bits allow re-construction of the original signal and error correction against scratches of the disc surface. Also, mass production of discs with high quality from a mother disc is possible by a simple moulding process [15].

A compact disc player is an optical decoding device that reproduces original information from a compact disc [3]. Information is written in a First-In-First-Out buffer. A typical compact disc player consists of an Optical Read Out Unit (or Optical Pick-up), a Radial Control Unit, a Focus Control Unit and a Rotation Speed Control Unit.

2.2.1 Optical Read Out Unit

An Optical Read Out Unit contains a laser diode (AlGaAs type), a semi-reflective mirror, a collimator lens, an objective lens and four photo-diodes. The laser diode generates a laser beam of suitable wavelength (0.76 to $0.82\mu m$, depending on the proportion of aluminium in the laser diode) which is then transformed to a parallel laser beam by the collimator lens after reflecting on the semi-reflective mirror. A single spot laser (Single Spot Mechanism) of diameter $1\mu m$ is focused on the disc by the objective lens. Three Spot Mechanisms exist as well but will not be discussed in this report. The objective lens can be adjusted vertically $2mm$ up and down by a vertical movement actuator. The vertical movement actuator is a coil wound around the objective lens and a cylindrical magnet. After the reflection of the laser beam on the reflective disc surface, the returning beam, which carries the

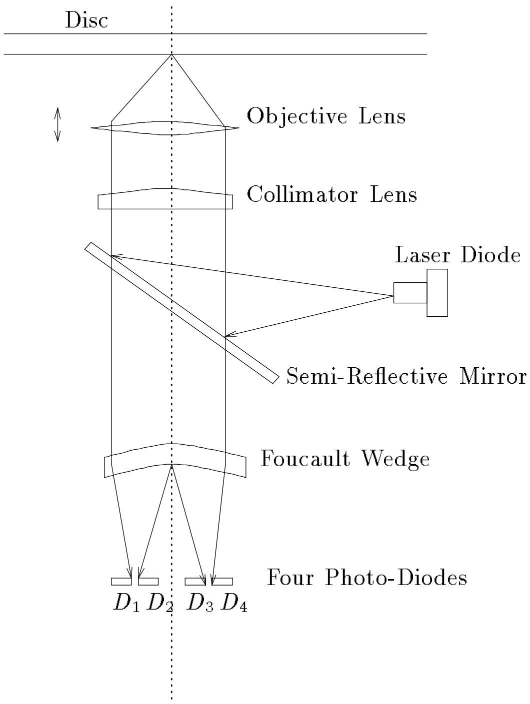

Figure 2.2: Optical Read Out Unit of Philips CD930

digital information, traces along the same path and then penetrates through the semi-reflective mirror to shine on the four photo-diodes via the Foucault wedge. The photo-diodes will then convert the visual signals into electrical signals (Figure 2.2).

2.2.2 Radial Control Unit

A Radial Control Unit consists of a radial actuator arm in which the Optical Read Out Unit is attached at one end (Figure 2.3). The other end of the radial actuator is a linear DC motor (coil and magnet) which is regulated by the fed electric current. The radial arm is initially positioned in the inner track and is gradually moved outwards. The radial actuator is basically a double integrator (as a transfer function from the input radial current to the spot position). A parasitic second order (damping) system with resonance frequency of approximately $3,700Hz$ is also included. The compromised bandwidth of the radial control loop is designed to be $500Hz$. In order to have good tracking of the reference digital signal, the laser spot should shine on a desire position with high accuracy. The allowable accuracy is $\pm 0.1\mu m$. However, standard errors such as imperfections in the disc (called Pickelschrammen), and eccentricity of the disc hole (up to $\pm 0.2mm$) can ruin

Figure 2.3: Schematics of the Mechanical and Optical Features of the Philips CD930

perfect tracking. As a result, feedback control of radial error with reduction factor 2,000 ($= 0.2mm/0.1\mu m$) is necessary.

2.2.3 Focus Control Unit

A Focus Control Unit consists of a focus actuator which is mounted on the top of the Optical Read Out Unit. The focus actuator is composed of an objective lens, leaf springs and a coil-magnet linear DC motor. The lens is placed in the coil, which is attached to the Optical Read Out Unit by two parallel leaf springs. The coil is embedded in a magnet to form the linear DC motor. The springs offer the possibility of a vertical movement of the objective lens, invoked by the linear DC motor. In order to avoid locking of the laser spot on the (reflective) hard protective layer during startup, the lens is first positioned close to the disc and is then slowly moved away. The motor is basically a second order (damping) system with resonance frequency of approximately $40Hz$. The bandwidth of the focus control loop is $800Hz$. Allowable focusing error is $\pm 2\mu m$. Nevertheless, large disturbances such as disc warp and up-and-down movement due to disc rotation (up to $\pm 0.5mm$) are common. A feedback control of focus error with reduction factor 250 ($= 0.5mm/2\mu m$) is required.

2.2.4 Rotation Speed Control Unit

The turntable rotates in the counterclockwise sense looking from the reading side. As the disc rotates and the radial arm moves outwards, optical data are read by the four photo-diodes. The read out speed of the digital data from the disc has to be kept nearly constant (scanning velocity 1.2 to $1.4ms^{-1}$) since the data density is constant over the whole disc. In order to maintain a constant read out speed, a controller has to be designed. The principle adopted by this rotation speed controller in Philips CD930 is that the First-In-First-Out information buffer is kept to be half filled. This forces the turntable to rotate gradually slower as the laser spot moves from the innermost position to the outermost position. The rotation speed is about $8Hz$ $(= 1.2ms^{-1}/(23mm * 2 * \pi))$ in the innermost position while it is about $3Hz$ $(= 1.2ms^{-1}/(58mm * 2 * \pi))$ at the outmost position. The read out speed is determined through comparison of the rate of the incoming data from the disc with a reference pulse generated by a quartz pulse.

A summary of standards of the Philips CD930 is given in Appendix A.

From now on to the end of this chapter, we will only concentrate on the control issues of radial error and focus error. Control of rotation speed will not be discussed in this report.

2.3 Control of Radial Error and Focus Error

The reflected laser beams on the four photo-diode sensors are, indeed, interference patterns in which light intensity depends on the vertical and horizontal position of the laser spot on the disc as compared with the desired focused position. However, *the absolute track and spot position are unknown.* Relative position between the absolute track and the laser spot can be estimated. *In order that an appropriate control of spot position and perfect focusing are possible, the controller should rely on the incoming "indicator signal" that changes its sign at zero when the errors increase from negative to positive.* Before constructing the "indicator signals", we firstly define radial position index and focus position index through the combinations of the four photo-diode currents. Define the radial position error index R_{error}, the focus position error index F_{error} and the sum signal CA as

$$\begin{aligned} R_{error} &:= (I_3 + I_4) - (I_1 + I_2) \\ F_{error} &:= (I_1 + I_4) - (I_2 + I_3) \\ CA &:= (I_1 + I_2) - (I_3 + I_4) \end{aligned}$$

where I_i, $i = 1, 2, 3, 4$ denotes the current generated from the photo-diode D_i (Figure 2.2). The indices R_{error} and F_{error} are nonlinear functions of the real spot position. However, their characteristics are linear near the origin. Further details will be discussed in the following subsections.

2.3.1 Radial Control

The radial position actuator is designed to follow the track movements and provide a sufficient positioning accuracy in spite of eccentricities and disturbances. The radial position error index is constructed by the so-called Push-Pull signal [3]. The radial position error index can be modelled as:

$$R_{error} = a + 2b \sin\left(\frac{\phi}{2}\right) \sin\left(\frac{2\pi\epsilon}{p}\right)$$

where

a	:	A DC term, resulting in a physical offset term, caused by a misplaced Foucault wedge in the Optical Read Out Unit. This offset can reach values in the same order of magnitude as the track.
b	:	The gain of the photo-diodes and other optical elements in the Optical Read Out Unit and also a function of the laser intensity emitted by the AlGaAs laser.
ϕ	:	Phase difference between the two components of the Push-Pull signal $R_{error} := (I_3 + I_4) - (I_1 + I_2)$. It is strongly dependent on the depth of the pits. Approximately, $\phi = \pi/2$.
ϵ	:	Physical control error ($\epsilon = x_{spot} - x_{track}$) where x_{spot} and x_{track} are defined as the distances from the center of the disc.
p	:	Distance between tracks, $1.6\mu m$ approximately.

Linearize the relation at $\epsilon = 0$ and with $\phi = \pi/2$, we have

$$R_{error} = a + \frac{2\sqrt{2}\pi b}{p} \cdot \epsilon.$$

Denote $R_{offset} := a$ and $K_{opt} := \frac{2\sqrt{2}\pi b}{p}$. Define the unbiased radial error signal RE by

$$RE := K_{opt} \cdot \epsilon.$$

The signal RE is an offset free signal. The characteristic is depicted as Figure 2.4. The Optical Read Out Unit is mounted at the end of the balanced radial actuator arm. The actuator is a DC motor without any spring restricting its rotation. When the actuator current I_{rad} is sent to the motor, the coil and magnet create a torque on the arm:

$$T_{arm} = K_{motor} \cdot I_{rad} \qquad [Nm]$$

Figure 2.4: The Characteristic of the RE signal

where T_{arm} is the torque, K_{motor} the gain, and I_{rad} the radial control current. On the other hand, the torque T_{arm} causes an angular acceleration which is inversely proportional to the moment of inertia of the arm

$$\ddot{\phi}_{arm} = \frac{T_{arm}}{J_{arm}} \qquad [rad/sec^2].$$

So, in the Laplace frequency domain, we have

$$\phi(s) = \frac{K_{motor}}{J_{arm}} \cdot \frac{I_{rad}(s)}{s^2}.$$

Define the transfer function from I_{rad} to ϕ as

$$H_{act} := \frac{\phi(s)}{I_{rad}(s)} = \frac{K_{motor}}{J_{arm}} \cdot \frac{1}{s^2}.$$

Owing to the fact that the radial arm has finite length, the movement of the Optical Read Out Unit across the tracks will not be perpendicular to the track direction as ϕ increases. From simple trigonometry (Figure 2.5), we have

$$\begin{aligned} x_{spot} &= \sqrt{[d - R\sin(\phi)]^2 + [R\cos(\phi)]^2} \qquad [m] \\ &= \sqrt{d^2 + R^2 - 2dR\sin(\phi)} \qquad [m] \end{aligned} \tag{2.1}$$

where R is the radius of the actuator arm, d the distance between the axis of the disc motor and the axis of the radial actuator motor and ϕ the rotation angle. Equation 2.1 can be linearized around any ϕ_0 to another x_{spot} as a linear function of ϕ:

$$x_{spot}(\phi) - x_{spot}(\phi_0) \approx -\frac{dR\cos(\phi_0)}{\sqrt{d^2 + R^2 - 2dR\sin(\phi_0)}} \cdot (\phi - \phi_0)$$

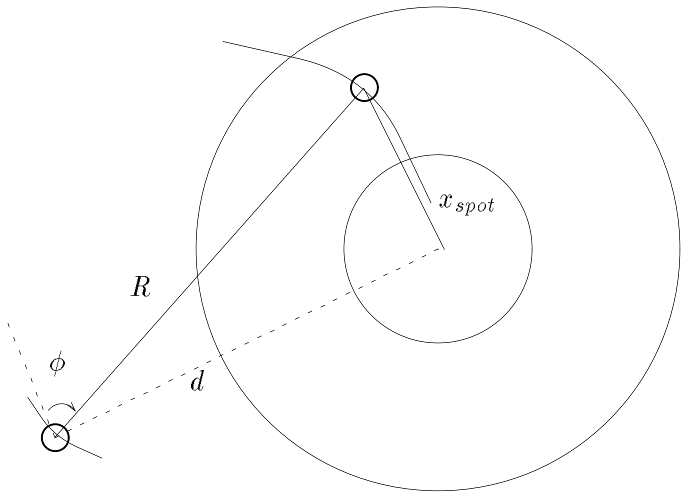

Figure 2.5: Dertermination of the Distance of the Spot from the Center of the Disc, x_{spot}, from the Geometry of the Actuator Design

For dynamic behaviour of the system at a certain time instant, the DC term is irrelevant and so

$$\triangle x_{spot}(\phi) = K_{arm} \cdot \triangle\phi$$

where

$$K_{arm} := -\frac{dR\cos(\phi_0)}{\sqrt{d^2 + R^2 - 2dR\sin(\phi_0)}}$$

with $\phi_0 \in (-15^o, 40^o)$ and $\triangle$ means infinitesimal changes (in x_{spot} and ϕ). So, the arm gain K_{arm} varies along the position of the position of the disc and its variation lies

$$R \cdot \cos(40^o) \le K_{arm} \le R$$

which, in turn, is equivalent to

$$0.77 \le \frac{K_{arm}}{R} \le 1.$$

Thus, the total transfer function of the radial position servo system from the actuator current I_{rad} to the unbiased error signal RE, when only movements of the spot relative to a fixed track is taken into account, is given by

$$H_{rad} := \frac{RE(s)}{I_{rad}(s)} = \frac{K_p}{s^2}$$

where the gain $K_p = \frac{K_{opt} \cdot K_{arm} \cdot K_{motor}}{J_{arm}}$. An actual dynamics also has a parasitic damping dynamics

$$H_{parasite} = \frac{\omega_0^2}{s^2 + 2\xi\omega_0 s + \omega_0^2}$$

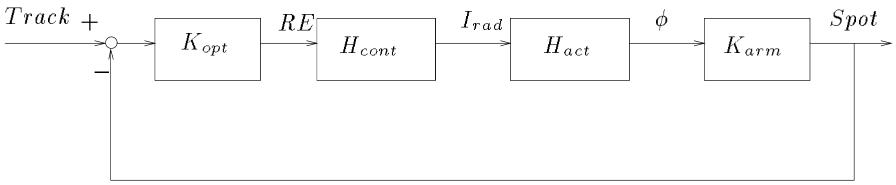

Figure 2.6: The Structure of the Radial Control Loop

where ω_0 is the undamped resonance frequency and ξ is the damping coefficient. The peak in the Bode plot of $H_{rad} \cdot H_{parasite}$ is the damped resonance frequency $\omega_n = \omega_0\sqrt{1-2\xi^2}$ (about $3,700Hz$). As we said before, neither the actual spot position nor the track position are known. Only the error signal RE, weighed by K_{opt}, is available for control action.

The actuator transfer function H_{rad} is a double integrator with poles on the imaginary axis and a constant phase lag of 180^o. In practice, a lead compensator is added to stabilize the plant (greater stability margin). In addition, the radial controller has a PI-section so as to reduce the DC-load disturbance (Figure 2.6). The transfer function of the controller is

$$H_{cont}(s) = K_{cont} \cdot \left(\frac{s\tau_i + 1}{s\tau_i}\right) \cdot \left(\frac{s\tau_d + 1}{s\tau_d/N + 1}\right).$$

In the Philips CD930 model, the zero of the PI is at $25Hz$ (that is, $\tau_i = 0.04$), the zero of the lead-lag is at $150Hz$ (that is, $\tau_d \approx 0.0067$) and the pole of the lead-lag is at $1,200Hz$ (that is, $N = 8$).

2.3.2 Focus Control

The control of focus depth is necessary in order to overcome inevitable disturbances such as the finger prints, irregularities in the disc height, the undulations of the surface and the un-orthogonal clamping of the disc. Similar to the radial unit, the focus motor is basically a second order lightly damped system with resonance frequency $40Hz$. The characteristic of the unbiased focus error FE is depicted in Figure 2.7. It is controlled by a Single-In-Single-Out controller, leading to a nominal bandwidth frequency of $800Hz$. This bandwidth may vary around the nominal value due to the production tolerances and optical aberrations. The focus controller has a lead segment in stabilizing the double integrator, and a PI section in giving a good servo behaviour for low frequency movements.

Figure 2.7: The Characteristic of the FE Signal

2.3.3 Practical Remarks

In practice, the parameters in transfer functions may vary in time, per disc and per CD player. For the Radial Control Unit, possible variations can occur in optical transfer function gain K_{opt}, arm transfer function gain K_{arm} and radial actuator gain $\frac{K_{motor}}{J_{arm}}$. Belows are given some detailed quantitative descriptions of the variations.

Variation of the optical transfer function gain

The transfer function of the relative movement of the spot out of the centre of the track to a photo-diode current is affected by a series of varying parameters:

- the shape, depth and slope of the pits on the disc;
- the intermediate track distance p;
- the optical qualities of the transparent layer on the disc;
- the optical transmission quality of the lenses;
- dust and other stains on the disc; and
- tolerances of fabrication of the optical elements, such as placement of the Foucault wedge and optical diodes.

These variations are stochastic and they are unpredictable for each disc and each player. Even during playing, their changes can be unpredictable. Empirically, the optical element has a total gain tolerance of $\pm 52\%$ whereas the disc related parameters may vary $\pm 40\%$.

Figure 2.8: Bode Plot of the Open Loop Transfer Function of the Controlled Radial Actuator

Variation of the arm transfer function gain

This is caused by the geometry of the arm actuator (as shown in Subsection 2.3.1). The angle with which the spot crosses the track directions varies as the spot moves from the innermost track to the outermost track. The gain variation of the arm is approximately $\pm 15\%$, due to this effect. It is a deterministic function which is related to the arm angle ϕ.

Variation of the radial actuator

It is affected by the gain of the motor K_{motor} and the variation of the moment of inertia J_{arm}. Overall variation of $\frac{K_{motor}}{J_{arm}}$ can reach $\pm 20\%$ empirically.

Based on computations in probability theory [6], the additive gain variation relative to the nominial parameter of the total set of parameter variations is about $\pm 80\%$. When the variation is presented as multiplicative type, the highest and the lowest possible gains give a variation factor of nine. In order words, the ratio of the real gain to the mean value is

$$\frac{1}{3} \leq \frac{K_{real}}{K_{mean}} \leq 3.$$

Owing to the variations in the radial gains, the bandwidth of the open loop transfer function may vary from $200Hz$ to $1,200Hz$ (Figure 2.8). This results in a poor phase margin and poor control performance. In order to solve the problem of constant bandwidth, the method of Automatic Gain Controller is employed. The idea of this method is that an external sine wobble of frequency $550Hz$ is injected. Owing to the plant dynamics, the wobble is changed in amplitude and in phase. This change provides a direct measure of the actual bandwidth.

Another practical remark is the acquisition of the unbiased radial error signal RE from the radial position error R_{error} for control purpose. The obtained R_{error} signal has a DC term due to asymmetric light intensity distributions of the reflected laser beams. This term may reach 50% of the maximum R_{error} signal. Compensation of offset can be achieved by the wobble method stated before. The offset term can be reduced to $\pm 0.01\mu m$, practically.

2.4 Repetitive Control in a CD Player

We have seen the possibilities of significant errors in the radial control loop and the focus control loop due to eccentricities and undulations of the un-orthogonal clamping of disc surface during rotation. In this particular disturbance rejection problem (that is, making the unbiased errors RE and FE small), the nature of these disturbances is "periodic". In fact, these "periodic" disturbances change their periods with the change of radial arm position as the rotation speed of the disc depends on the radial arm position. The period becomes larger when the angular speed of disc rotation decreases according to the outward movement of the radial arm. However, the "period" can be treated as constant in a short period of time at any particular instant. This is how repetitive control comes into the picture.

Given a finite dimensional linear time invariant system G, suppose the system is fed with the class of all periodic input signals with the same period T, say. Denote $\mathcal{P}_T$ the set of all periodic functions of period T over the time interval $[0, \infty)$. We are aiming to make the output of the system over a certain subclass of $\mathcal{W}_T$ (that is, with finite "norm") "small" in some sense. We measure the signals by the so-called average power, a semi-norm (but becomes a norm in $\mathcal{P}_T$). We cannot use the traditional 2-norm in $\mathcal{L}^2[0, \infty)$ because periodic signals have infinite 2-norms. On the other hand, periodic functions of period T are composed of infinitely many harmonics, namely of frequencies $\frac{2\pi k}{T}$ where k is an integer. We are going to design a stabilizing feedback controller so that the output of the system G over that subclass of $\mathcal{P}_T$ is "small" for all harmonics.

In case of disturbance rejection in our CD player model, the inputs are the "periodic" disturbances while the output are the tracking errors. Actually, we have to modify the parameters of the stabilizing controller adaptively according to the change of the radial arm position. This can be done with the need of the angular speed of the disc, which can be determined directly or indirectly.

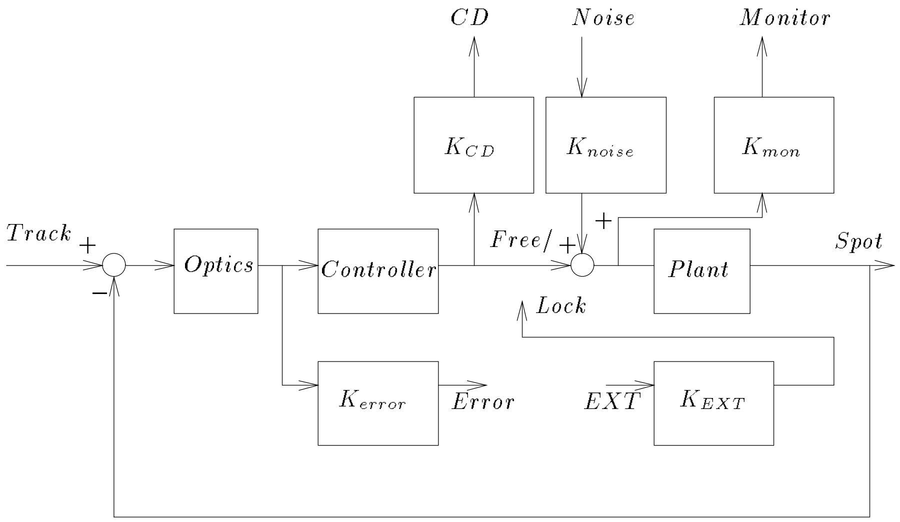

Figure 2.9: Block Diagram of Control Loops in Philips CD930

The actual control rig for radial loop and focus loop in the Philips CD930 model can be described in Figure 2.9. For both loops, the actual references are unknown but the error signals coming out from the optics can be fed into the standard internal controller. However, both loops can also be switched independently from the internal controller EXT to an external controller via a 'free/lock'. We are going to implement our designed analog controller by dSPACE together with a sampler and a hold. One of the main advantages of using dSPACE is that the parameters and even the structures of the external controller can be implemented easily and conveniently in a computer programmable way. This digital implementation will be "close" to an analog controller and intersample behaviours have to be taken into account. These theoretical issues will be studied in next chapter.

Chapter 3

Repetitive Control

3.1 Introduction

Repetitive control has been proposed for the purpose of tracking unknown periodic reference commands and/or rejecting disturbance signals in a system in which the period is known. Applications include machine tool chatter control [19], tool positioning in noncircular machining [24], tracking in disk-file actuator [21, 22, 23] and material testing [20, 17]. There has been intense research on this theory. The basic idea of the design strategy is the Internal Model Principle [8].

Repetitive controllers can be classified into two types according to their nature: continuous-time and discrete-time. These controllers should have their internal model components included (namely, $1/(1-\exp(-sT))$ for continuous-time periodic signal of period T and $1/(1-z^N)$ for discrete-time periodic signal of period N) in order to have perfect tracking and/or disturbance rejection of periodic signals. For the continuous-time case, the controller is infinite dimensional so that all the harmonics (that is, of frequencies $j\frac{2\pi}{T}k,\ k=0,1,...$) can be perfectly controlled. It turns out that the class of the systems to be stabilized by such controllers is quite limited [9, 10, 11], namely, those systems whose transfer functions have relative degree zero. We also know that this stabilization will not be robust to any small time delays so that, practically, it is not possible to reject arbitary periodic disturbances perfectly even for those systems with relative degree zero case. In order to compromise the dilemma of perfect tracking/rejection and the limited class of systems, people [9, 11] weighted the delay term $\exp(-sT)$ by a low-pass filter having infinity-norm less than or equal to unity. This modified repetitive controller can be applied to low-pass filtered input signals. Repetitive control of continuous-time systems can also be controlled by discrete-time controller with the help of a sampler and a hold. Work on this sampled-data repetitive control was begun in this decade [1, 2, 12, 13, 14, 4]. Lifting technique was adopted in sampled-data repetitive control. On the other hand, discrete-time repetitive control and its applications were studied separately in the past few decades [21, 24, 22, 23].

3.2 Mathematical Preliminaries

We begin with several mathematical definitions. Denote $\mathbb{R}_+$ the interval $[0, \infty)$ in $\mathbb{R}$, $\mathcal{L}(\mathbb{R}_+, \mathbb{R}^p)$ the linear space of all functions from $\mathbb{R}_+$ to the Euclidean space $\mathbb{R}^p$, $\mathbb{Z}_+$ the set of all non-negative integers, and $\ell(\mathbb{Z}_+, \mathbb{R}^p)$ the set of all sequences in $\mathbb{R}^p$. A continuous-time signal w in $\mathcal{L}(\mathbb{R}_+, \mathbb{R}^p)$ is said to be *periodic* of period T if

$$w(t+T) = w(t), \qquad t \geq 0.$$

Define the *average power* (or simply *power*) [5] of $w \in \mathcal{L}(\mathbb{R}_+, \mathbb{R}^p)$ by

$$pow(w) := \left(\lim_{\gamma \to \infty} \frac{1}{\gamma} \int_0^\gamma w(t)' w(t)\, dt \right)^{1/2}$$

where the prime $'$ denotes the transpose. Define the subspace in $\mathcal{L}(\mathbb{R}_+, \mathbb{R}^p)$

$$\mathcal{W}_T := \{ w \in \mathcal{L}(\mathbb{R}_+, \mathbb{R}^p) : w \text{ is periodic of period } T,\ pow(w) < \infty \}.$$

Analoguously, we can define similar concepts for discrete-time signals. A discrete-time signal ω in $\ell(\mathbb{Z}_+, \mathbb{R}^p)$ is said to be *periodic* of period m if

$$\omega(n+m) = \omega(n), \qquad n \geq 0.$$

Average power (or simply *power*) of $\omega \in \ell(\mathbb{Z}_+, \mathbb{R}^p)$ is defined as

$$pow(\omega) := \lim_{N \to \infty} \left(\frac{1}{N} \sum_{n=0}^{N-1} \omega(n)' \omega(n) \right)^{1/2}.$$

Define the subspace in $\ell(\mathbb{Z}_+, \mathbb{R}^p)$

$$\Omega_m = \{ \omega \in \ell(\mathbb{Z}_+, \mathbb{R}^p) : \omega \text{ is periodic of period } m,\ pow(\omega) < \infty \}.$$

From now on, we use the same notation of power in acting on continuous-time signals and discrete-time signals. In general, these definitions of powers in continuous-time case and in discrete-time case (namely, $pow(w)$ and $pow(\omega)$) are semi-norms but they become genuine norms if they are acting on the subspaces $\mathcal{W}_T$ of $\mathcal{L}(\mathbb{R}_+, \mathbb{R}^p)$ and Ω_m of $\ell(\mathbb{Z}_+, \mathbb{R}^p)$ respectively. It is noted that the powers for which $w \in \mathcal{W}_T$ and $\omega \in \Omega_m$ can be calculated by the following simple relations:

$$pow(w) = \left(\frac{1}{T} \int_0^T w(t)' w(t)\, dt \right)^{1/2}$$

and

$$pow(\omega) = \left(\frac{1}{m} \sum_{n=0}^{m-1} \omega(n)' \omega(n) \right)^{1/2}$$

if $pow(w)$ exists. Representing a periodic function of period T as its Fourier series is a convenient way for our analysis [7].

Definition 3.2.1 (Folland [7]). *Suppose* $f : [0, \infty) \longrightarrow \mathbb{R}^p$ *is periodic of period* T *and (Lebesgue) integrable over* $[0, T]$. *The series*

$$\sum_{k=-\infty}^{\infty} a_k e^{j \frac{2\pi}{T} kt}$$

is called the Fourier series of f *where*

$$a_k := \frac{1}{T} \int_0^T f(t) e^{-j \frac{2\pi}{T} kt}\, dt$$

are called the Fourier coefficients of f.

Denote the partial sum of Fourier series as

$$S_N^f(t) := \sum_{k=-N}^{N} a_n e^{j \frac{2\pi}{T} kt}.$$

A function f defined on an interval $[a, b]$ is said to be piecewise C^1 if f and its first derivative are piecewise continuous on $[a, b]$. The following Proposition [7] tells about the validity of expressing a function as its Fourier series.

Proposition 3.2.2 (Folland [7]). *If* $f : [0, \infty) \longrightarrow \mathbb{R}^p$ *is periodic of period* T *and piecewise* C^1 *on* $\mathbb{R}_+$, *then*

$$\lim_{N \to \infty} S_N^f(t) = \frac{1}{2} [f(t-) + f(t+)]$$

for every $t \geq 0$. *In particular,* f *will be equal to its Fourier series if* f *is also continuous.*

Lemma 3.2.3. *Suppose $w \in \mathcal{L}(\mathbb{R}_+, \mathbb{R}^p)$ can be written as a sum $w = w_1 + w_2$ where w_1 is in $\mathcal{L}^2(\mathbb{R}_+, \mathbb{R}^p)$ and w_2 is in $\mathcal{W}_T$. Then*

$$pow(w) = pow(w_2)$$

if all powers exist. Similar result holds for sequences in $\ell(\mathbb{Z}_+, \mathbb{R}^p)$. That is,

$$pow(\omega) = pow(\omega_2)$$

if $\omega = \omega_1 + \omega_2$ where ω_1 is in $\ell^2(\mathbb{Z}_+, \mathbb{R}^p)$, ω_2 is in Ω_m and all power exists.

Proof. Use the definition of power and use Cauchy-Schwarz inequality to bound the cross-term. $\square$

For periodic discrete-time signals in Ω_m, we define the discrete Fourier transform equations [16]:

$$\begin{array}{llll} \text{Analysis Equation} & \tilde{\omega}(k) & = \displaystyle\sum_{n=0}^{m-1} \omega(n)\lambda_n^{-k}, & k \geq 0 \\ \text{Synthesis Equation} & \omega(n) & = \displaystyle\frac{1}{m}\sum_{k=0}^{m-1} \tilde{\omega}(k)\lambda_k^{n}, & n \geq 0, \end{array}$$

where

$$\lambda_k := e^{j\frac{2\pi}{m}k}, \qquad k = 0, 1, ..., m-1.$$

For a general (not necessarily periodic) discrete-time signal $\psi(n)$, define the λ-transform (where $\lambda = z^{-1}$) by

$$\hat{\psi}(\lambda) = \sum_{n=0}^{\infty} \psi(n)\lambda^n.$$

Making use of the Synthesis Equation, we can show that the λ-transform of a periodic signal $\omega(n)$ in Ω_m can be rewritten as

$$\hat{\omega}(\lambda) = \frac{1}{m}\sum_{k=0}^{m-1} \frac{\tilde{\omega}(k)}{1 - \lambda\lambda_k}.$$

Lemma 3.2.4 (Langari and Francis [13]). *For $\omega(n)$ periodic of period m*

$$pow(\omega) = \frac{1}{m}\left(\sum_{k=0}^{m-1} \tilde{\omega}(k)^*\tilde{\omega}(k)\right)^{\frac{1}{2}}.$$

Proof. Use the relation

$$pow(\omega) = \left(\frac{1}{m} \sum_{n=0}^{m-1} \omega(n)' \omega(n) \right)^{1/2}$$

for $\omega \in \Omega_m$, the Synthesis Equation and the fact

$$\sum_{n=0}^{m-1} (\lambda_k^* \lambda_l)^n = \begin{cases} 0, & k \neq l \\ m, & k = l \end{cases}.$$

□

We will look at the behaviours of a *stable* discrete-time system when it is excited by periodic discrete-time inputs. Consider a stable FDLTI discrete-time system Φ with input $\omega \in \Omega_m$, output ψ and transfer function $\hat{\Phi}(\lambda)$. For periodic input $\omega \in \Omega_m$, we have

$$\hat{\omega}(\lambda) = \frac{1}{m} \sum_{k=0}^{m-1} \frac{\tilde{\omega}(k)}{1 - \lambda \lambda_k}.$$

So,

$$\begin{aligned} \hat{\psi}(\lambda) &= \hat{\Phi}(\lambda) \hat{\omega}(\lambda) \\ &= \frac{1}{m} \sum_{k=0}^{m-1} \frac{\hat{\Phi}(\lambda) \tilde{\omega}(k)}{1 - \lambda \lambda_k}. \end{aligned}$$

We can decompose the output $\hat{\psi}(\lambda)$ into the steady state component and the transient component:

$$\begin{aligned} \hat{\psi}(\lambda) &= \hat{\psi}_{ss}(\lambda) + \hat{\psi}_{tr}(\lambda) \\ \hat{\psi}_{ss}(\lambda) &:= \frac{1}{m} \sum_{k=0}^{m-1} \frac{\hat{\Phi}(\lambda_k^{-1}) \tilde{\omega}(k)}{1 - \lambda \lambda_k} \\ \hat{\psi}_{tr}(\lambda) &:= \frac{1}{m} \sum_{k=0}^{m-1} \frac{\hat{\Phi}(\lambda) - \hat{\Phi}(\lambda_k^{-1})}{1 - \lambda \lambda_k} \tilde{\omega}(k). \end{aligned}$$

The transient part $\hat{\psi}_{tr}$ is analytic in the closed unit disk since the unstable poles in the denominator are cancelled by zeros in the numerator. Therefore, by Final Value Theorem, $\psi_{tr}(k)$ tends to zero as k tends to infinity. On the other hand, $\hat{\psi}_{ss}(\lambda)$ is a periodic signal of period m with $\tilde{\psi}_{ss}(k) = \hat{\Phi}(\lambda_k^{-1}) \tilde{\omega}(k)$ and

$$\psi_{ss}(k) = \frac{1}{m} \sum_{l=0}^{m-1} \hat{\Phi}(\lambda_l^{-1}) \tilde{\omega}(l) \lambda_l^k.$$

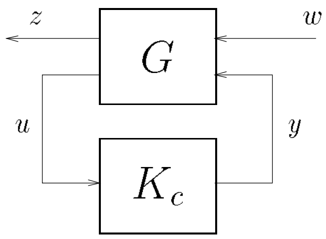

Figure 3.1: General Framework

As a result, ψ approaches to a steady state ψ_{ss}. An advantage of using power in measuring the "size" of the output rather than using the norm of the steady state component in the output [13] is that we do not need to compute the steady state explicitly and both quantities (that is, $pow(\psi)$ and $pow(\psi_{ss})$) will be the same (which will be proved in the next section [13]).

3.3 Problem Formulation

Given a FDLTI continuous-time system G with a minimal realization

$$\hat{G}(s) = \left[\begin{array}{c|cc} \overline{A} & \overline{B}_1 & \overline{B}_2 \\ \hline \overline{C}_1 & \overline{D}_{11} & \overline{D}_{12} \\ \overline{C}_2 & \overline{D}_{21} & \overline{D}_{22} \end{array}\right].$$

Exogeneous input w in $\mathcal{W}_T$ consists of periodic reference and/or disturbance signals of period T and the output z is all the errors. The controller input and the controller output are denoted by u and y respectively. K_c is the continuous-time controller to be designed so that the whole system is internally stable and the power of the error z is minimized (Figure 3.1). Denote by $\mathcal{C}$ the class of all FDLTI controllers (the same notation for continuous-time case or discrete-time case) for which the system is internally stable.

Definition 3.3.1. *Let P be a stable FDLTI continuous-time system. Define its induced power over all continuous-time periodic signals of period T by*

$$||P||_{\mathcal{W}_T} := \sup_{u \in \mathcal{W}_T,\ pow(u) \neq 0} \frac{pow(P * u)}{pow(u)}$$

where $*$ denotes the convolution integral. Similarly, we define the induced power of a stable FDLTI discrete-time system Φ over all discrete-time periodic signals of period m as

$$||\Phi||_{\Omega_m} := \sup_{\omega \in \Omega_m,\ pow(\omega) \neq 0} \frac{pow(\Phi * \omega)}{pow(\omega)}$$

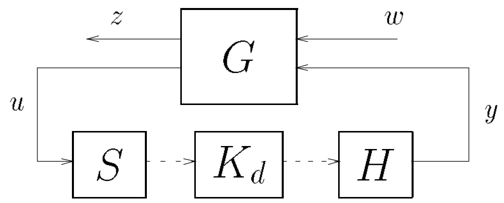

Figure 3.2: Sampled-Data Digital Control

where $*$ denotes the convolution sum.

We use the same notation $*$ for convolutions with no ambiguity. The induced power of a stable system is dependent on the period (T or m). These definitions of induced power can be interpreted as the power of the errors in the worst case for inputs of unit power.

There are two approaches in designing the stabilizing continuous-time controllers K_c, namely analog controller design and sampled-data digital controller design. We will only deal with sampled-data digital controller design in the remaining of this chapter. For the digital case, the controller input u has to be sampled by a sampler S before feeding into the controller whereas the digital signal just coming out from the controller will be converted to an analog signal via a hold H (Figure 3.2). Note that this digital controller design is a hybrid type (that is, continuous-time system input/output but with discrete-time controller input/output). This hybrid nature is problematic because the whole controller ($K_c = SK_dH$) has to be of a certain form and it is *not* time invariant. In fact it is T-periodic (that is, a time shift of T in the controller input gives the same controller output). Suppose we are looking at an approximate discrete-time system. *We will model the input w as an output of a fast zero order hold H_f and the output z is looked through a fast sampler S_f that is synchronized with H_f.*

Let us formulate our sampled-data optimal repetitive control problem. Consider the class $\mathcal{W}_T$ of all periodic functions of period T. Let h be the sampling period of the sampler S and hold H around the controller with $T = Mh$ where M is a positive integer. Suppose the fast sampler S_f and the fast hold H_f are having the same period $\frac{h}{N}$ where N is a designed parameter. Intersample points behaviours will be taken into account. So, the input discrete-time signal ω will have to be periodic with period MN since

$$T = Mh = MN(\frac{h}{N}).$$

In other words, w would be in $\mathcal{W}_T$ if ω is in Ω_{MN}. The hybrid will become

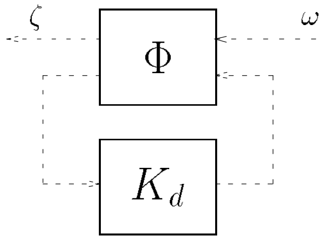

Figure 3.3: Two-Rate Discrete-Time System

a two-rate discrete-time system (Figure 3.3) where

$$\Phi := \begin{bmatrix} S_f & 0 \\ 0 & S \end{bmatrix} G \begin{bmatrix} H_f & 0 \\ 0 & H \end{bmatrix}.$$

This leads to the following *sampled-data optimal repetitive control problem*:

$$\min_{K_d \in \mathcal{C}} ||\mathcal{F}_l(\Phi, K_d)||_{\Omega_{MN}}. \tag{3.1}$$

Proposition 3.3.2 (Langari and Francis [13]). *Suppose $K_d \in \mathcal{C}$. Then for the sampled data setup (figure 3.3) and for each $\omega \in \Omega_{MN}$, there exist unique signals ζ_{ss} in Ω_{MN} and ζ_{tr} in $\ell^2(\mathbb{Z}_+, \mathbb{R}^p)$ so that the output $\zeta = \zeta_{ss} + \zeta_{tr}$.*

Proof. Refer to Theorem 2 in Langari's technical report [13]. □

In view of Lemma 3.2.3 and Proposition 3.3.2, the numerator in the definition of power of a discrete-time system Definition 3.3.1 can be replaced by $pow(\zeta_{ss})$. Moreover, the power of a discrete-time system depends only on its values at finitely many frequencies (that is, the harmonic frequencies of the discrete-time signals being tackled):

Theorem 3.3.3 (Langari and Francis [13]). *For any FDLTI discrete-time system Ψ, its induced power over the class Ω_m can be calculated by*

$$||\Psi||_{\Omega_m} = \max_{0 \le k \le m-1} \overline{\sigma}[\hat{\Psi}(\lambda_k)].$$

Proof. Let ζ be the output of $\omega \in \Omega_m$ through the system Ψ. Then

$$\begin{aligned} pow(\zeta)^2 &= pow(\zeta_{ss})^2 \\ &= \frac{1}{m^2} \sum_{k=0}^{m-1} \tilde{\zeta}_{ss}(k)^* \tilde{\zeta}_{ss}(k) \\ &= \frac{1}{m^2} \sum_{k=0}^{m-1} [\hat{\Psi}(\lambda_k^{-1})\tilde{\omega}(k)]^*[\hat{\Psi}(\lambda_k^{-1})\tilde{\omega}(k)] \end{aligned}$$

$$
\begin{aligned}
&\leq \frac{1}{m^2}\sum_{k=0}^{m-1}\overline{\sigma}[\hat{\Psi}(\lambda_k)]^2[\tilde{\omega}(k)^*\tilde{\omega}(k)] \\
&\leq \left(\max_{0\leq k\leq m-1}\overline{\sigma}[\hat{\Psi}(\lambda_k^{-1})]^2\right)\frac{1}{m^2}\sum_{k=0}^{m-1}\tilde{\omega}(k)^*\tilde{\omega}(k) \\
&= \max_{0\leq k\leq m-1}\overline{\sigma}[\hat{\Psi}(\lambda_k)]^2\ pow(\omega)^2.
\end{aligned}
$$

Thus,

$$
||\Psi||_{\Omega_m} \leq \max_{0\leq k\leq m-1}\overline{\sigma}[\hat{\Psi}(\lambda_k)].
$$

In order to prove that $||\Psi||_{\Omega_m}$ actually achieves the upper bound, it is sufficient to consider the vector $\tilde{\omega}_{max}$ in which $\overline{\sigma}[\hat{\Psi}(\lambda_{k_{max}}^{-1})]$ is maximum over all k and $|\hat{\Psi}(\lambda_{k_{max}}^{-1})\tilde{\omega}_{max}|$ achieves its maximum Euclidean norm. Setting

$$
\tilde{\omega}(k) = \begin{cases} \tilde{\omega}_{max}, & k = k_{max} \\ 0, & \text{else} \end{cases}
$$

as the input will do. $\square$

This two-rate discrete-time system (with rates MN and M) can be converted to a single-rate discrete-time system by the Lifting Technique [13]. Define the lifting operator $L : \ell(\mathbb{Z}_+, \mathbb{R}^p) \longrightarrow \ell(\mathbb{Z}_+, \mathbb{R}^{Np})$ by

$$
(L\omega)(k) = \begin{bmatrix} \omega(kN) \\ \omega(kN+1) \\ \vdots \\ \omega(kN+N-1) \end{bmatrix}.
$$

So, if a signal ω has a period MN, its lifted signal $L\omega$ has period M. Note that the lifted signal has dimension N times more. The inverse of lifting operator $L^{-1} : \ell(\mathbb{Z}_+, \mathbb{R}^{Np}) \longrightarrow \ell(\mathbb{Z}_+, \mathbb{R}^p)$ can be defined by

$$
L^{-1}\begin{bmatrix} \omega(kN) \\ \omega(kN+1) \\ \vdots \\ \omega(kN+N-1) \end{bmatrix} = \omega(k).
$$

Obviously, L (or L^{-1}) maps periodic signals of period MN (or M) to periodic signals of period M (or MN). Moreover, the power norm of these periodic signals will be scaled up (or down) under L (or L^{-1}) by a factor of $\sqrt{N}$ (or $1/\sqrt{N}$). This can be observed by the fact

$$
pow(L\omega)^2 = \frac{1}{M^2}\sum_{k=0}^{M-1}(L\omega)(k)'(L\omega)(k)
$$

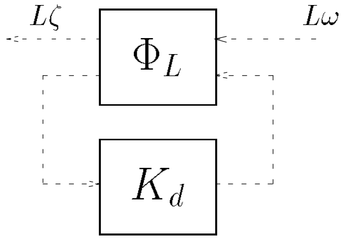

Figure 3.4: Single-Rate Lifted System

$$
\begin{aligned}
&= \frac{1}{M^2}\sum_{k=0}^{M-1}\begin{bmatrix}\omega(kN)\\ \omega(kN+1)\\ \vdots\\ \omega(kN+N-1)\end{bmatrix}'\begin{bmatrix}\omega(kN)\\ \omega(kN+1)\\ \vdots\\ \omega(kN+N-1)\end{bmatrix}\\
&= \frac{1}{M^2}\sum_{k=0}^{M-1}\sum_{l=0}^{N}\omega(kN+l)'\omega(kN+l)\\
&= \frac{1}{M^2}\sum_{i=0}^{MN-1}\omega(i)'\omega(i)\\
&= N\ pow(\omega)^2.
\end{aligned}
$$

That is,

$$pow(L\omega) = \sqrt{N}\ pow(\omega).$$

Introducing the lifting operator to the previous two-rate discrete-time system (Figure 3.3), we arrive at a single-rate system. The mapping from $L\omega \in \Omega_M$ to the output $L\zeta \in \Omega_M$ is given by

$$L\mathcal{F}_l(\Phi, K_d)L^{-1} = \mathcal{F}_l(\Phi_L, K_d)$$

where the new matrix Φ_L is equal to

$$\Phi_L := \begin{bmatrix} L & 0\\ 0 & I\end{bmatrix}\Phi\begin{bmatrix} L^{-1} & 0\\ 0 & I\end{bmatrix}. \tag{3.2}$$

The state-space realization for $\hat{\Phi}_L$ can be found in Appendix B. Observe that the lifted system has the same induced power as the original one, namely

$$||\mathcal{F}_l(\Phi, K_d)||_{\Omega_{MN}} = ||\mathcal{F}_l(\Phi_L, K_d)||_{\Omega_M}.$$

The resulting single-rate lifted system (Figure 3.4) is linear and time invariant so that classical $\mathcal{H}^\infty$ techniques [25] can be applied for stabilizing controllers design.

3.4 Design Procedure

We have seen in the past section that an optimal control problem is arrived in order to have error minimization for arbitary periodic signals of period T [13]. With the help of Theorem 3.3.3, the optimal problem can be rewritten as:

$$\min_{K_d \in \mathcal{C}} \max_{0 \le k \le M-1} \overline{\sigma}[\mathcal{F}_l(\hat{\Phi}_L, \hat{K}_d)(\lambda_k)]$$

where Φ_L is given by 3.2 and $\lambda_k = e^{j\frac{2\pi}{M}k}$.

In order to find all the solution of this minimax problem, we firstly characterize all the stabilizing controllers K_d in $\mathcal{C}$. Suppose

$$\hat{\Phi}_L(\lambda) = \left[\begin{array}{c|cc} A & B_1 & B_2 \\ \hline C_1 & D_{11} & D_{12} \\ C_2 & D_{21} & D_{22} \end{array}\right]$$

is the state space realization of the lifted system Φ_L defined in the previous section. Then all the stabilizing controllers [25] can be represented as $\hat{K}_d = \mathcal{F}_l(\hat{J}, \hat{Q})$ where

$$\hat{J}(\lambda) = \left[\begin{array}{c|cc} A + B_2F + HC_2 + HD_{22}F & -H & B_2 + HD_{22} \\ \hline F & 0 & I \\ -(C_2 + D_{22}F) & I & -D_{22} \end{array}\right]$$

in which F and H are chosen so that $A + B_2F$ and $A + HC_2$ are stable, $\hat{Q}$ is stable and $I + D_{22}\hat{Q}(\infty)$ is non-singular. As a result, the transfer function from $L\omega$ to $L\zeta$ is given by

$$T_{(L\zeta)(L\omega)} = \mathcal{F}_l(\hat{\Phi}_L, \hat{K}_d) = \mathcal{F}_l(\mathcal{S}(\hat{\Phi}_L, \hat{J}), \hat{Q}).$$

The star product

$$\mathcal{S}(\hat{\Phi}_L, \hat{J}) = \begin{bmatrix} \hat{\phi}_{11} & \hat{\phi}_{12} \\ \hat{\phi}_{21} & 0 \end{bmatrix}$$

can be calculated easily and hence

$$T_{(L\zeta)(L\omega)} = \hat{\phi}_{11}(\lambda) + \hat{\phi}_{12}(\lambda)\hat{Q}(\lambda)\hat{\phi}_{21}(\lambda)$$

where the $\hat{\phi}$'s are given by

$$\begin{aligned} \hat{\phi}_{11}(\lambda) &= \left[\begin{array}{cc|c} A + B_2F & B_2F & B_1 \\ 0 & A + HC_2 & -B_1 - HD_{21} \\ \hline C_1 + D_{12}F & D_{12}F & D_{11} \end{array}\right] \\ \hat{\phi}_{12}(\lambda) &= \left[\begin{array}{c|c} A + B_2F & B_2 \\ \hline C_1 + D_{12}F & D_{12} \end{array}\right] \end{aligned}$$

$$\hat{\phi}_{21}(\lambda) \quad = \quad \left[\begin{array}{c|c} A + HC_2 & B_1 + HD_{21} \\ \hline C_2 & D_{21} \end{array}\right].$$

Then, in view of Theorem 3.3.3, the sampled-data optimal repetitive control problem becomes

$$\min_{\hat{Q}(\lambda)\ stable} \max_{0 \le k \le M-1} \overline{\sigma}[\hat{\phi}_{11}(\lambda_k) + \hat{\phi}_{12}(\lambda_k)\hat{Q}(\lambda_k)\hat{\phi}_{21}(\lambda_k)]. \tag{3.3}$$

This problem can be solved as follows:

Lemma 3.4.1 (Langari and Francis [13]). *A minimizing solution Q for the problem 3.3 is*

$$\hat{Q}(\lambda) = \sum_{n=0}^{M-1} \tilde{r}(n)\lambda^n$$

where

$$\tilde{r}(n) = \frac{1}{M}\sum_{k=0}^{M-1} r(k)\lambda_k^{-n},$$

(that is, $\tilde{r}(k)$ is the one-Mth of the discrete Fourier transform of $r(n)$) and $r(k)$ solves

$$\min_{r(k)} \overline{\sigma}[\hat{\phi}_{11}(\lambda_k) + \hat{\phi}_{12}(\lambda_k)r(k)\hat{\phi}_{21}(\lambda_k)], \qquad k = 0, 1, ..., M-1.$$

Proof. The minimum in problem 3.3 is in general no smaller than

$$\min_{r(0),...,r(M-1)} \max_{0 \le k \le M-1} \overline{\sigma}[\hat{\phi}_{11}(\lambda_k) + \hat{\phi}_{12}(\lambda_k)r(k)\hat{\phi}_{21}(\lambda_k)]. \tag{3.4}$$

In particular, they are equal if there is a stable $\hat{Q}(\lambda)$ that satisfies

$$\hat{Q}(\lambda_k) = r(k), \qquad k = 0, ..., M-1.$$

On the other hand, since the optimization variables are independent to each other, the minimax operator can be interchanged and problem 3.4 is equivalent to

$$\max_{0 \le k \le M-1} \min_{r(0),...,r(M-1)} \overline{\sigma}[\hat{\phi}_{11}(\lambda_k) + \hat{\phi}_{12}(\lambda_k)r(k)\hat{\phi}_{21}(\lambda_k)],$$

which, in turn, is equivalent to

$$\max_{0 \le k \le M-1} \min_{r(k)} \overline{\sigma}[\hat{\phi}_{11}(\lambda_k) + \hat{\phi}_{12}(\lambda_k)r(k)\hat{\phi}_{21}(\lambda_k)]. \tag{3.5}$$

Hence, if one interpolates the points $r(k)$, which solves the minimization problem 3.4, with a polynomial, then a stable optimal $\hat{Q}(\lambda)$ is obtained. $\square$

It remains to solve the M individual minimization problems in 3.5. These M minimization problems share the same form

$$\min_X \ \overline{\sigma}(E_1 + E_2 X E_3),$$

where E_1, E_2, E_3 and X are complex matrices. This problem has a closed-form solution via the singular value decomposition. Denote by $\dagger$ the Moore-Penrose generalized inverse.

Lemma 3.4.2 (Langari and Francis [13]). *Let*

$$E_2 = U_2 \begin{bmatrix} \Sigma_2 & 0 \\ 0 & 0 \end{bmatrix} V_2^*$$

and

$$E_3 = U_3 \begin{bmatrix} \Sigma_3 & 0 \\ 0 & 0 \end{bmatrix} V_3^*$$

be the singular value decompositions of E_2 and E_3. Define

$$\overline{E}_1 := U_2^* E_1 V_3 \text{ and } \overline{X} := V_2^* X U_3$$

and write

$$\overline{E}_1 = \begin{bmatrix} \overline{E}_{11} & \overline{E}_{12} \\ \overline{E}_{21} & \overline{E}_{22} \end{bmatrix}$$

as the natural partitions induced by the product

$$\begin{bmatrix} \Sigma_2 & 0 \\ 0 & 0 \end{bmatrix} \overline{X} \begin{bmatrix} \Sigma_3 & 0 \\ 0 & 0 \end{bmatrix}.$$

Then

$$\min_X \ \overline{\sigma}(E_1 + E_2 X E_3) = \max \left(\overline{\sigma} \begin{bmatrix} \overline{E}_{12} \\ \overline{E}_{22} \end{bmatrix}, \overline{\sigma} \begin{bmatrix} \overline{E}_{21} & \overline{E}_{22} \end{bmatrix} \right) =: \alpha$$

and a minimizing solution is given by

$$X = V_2 \begin{bmatrix} \Sigma_2^{-1} W \Sigma_3^{-1} & 0 \\ 0 & 0 \end{bmatrix} U_3^*$$

where

$$W := -\overline{E}_{11} - \overline{E}_{12} \overline{E}_{22}^* (\alpha^2 I - \overline{E}_{22} \overline{E}_{22}^*)^\dagger \overline{E}_{21}.$$

Proof. Set $Y := E_1 + E_2 X E_3$ and $\overline{Y} := U_2^* Y V_3$. Since matrices U_2 and V_3 are unitary, we have

$$\overline{\sigma}(\overline{Y}) = \overline{\sigma}(Y).$$

It is easy to verify that

$$\overline{Y} = \begin{bmatrix} Z & \overline{E}_{12} \\ \overline{E}_{21} & \overline{E}_{22} \end{bmatrix}$$

where

$$Z = \overline{E}_{11} + \begin{bmatrix} \Sigma_2 & 0 \end{bmatrix} \overline{X} \begin{bmatrix} \Sigma_3 \\ 0 \end{bmatrix}.$$

From the result in [25], the minimizing value is

$$\alpha := \max \left(\overline{\sigma} \begin{bmatrix} \overline{E}_{12} \\ \overline{E}_{22} \end{bmatrix}, \overline{\sigma} \begin{bmatrix} \overline{E}_{21} & \overline{E}_{22} \end{bmatrix} \right)$$

and a minimizing solution is given by

$$Z_{min} = -\overline{E}_{12}\overline{E}_{22}^{*}(\alpha^2 I - \overline{E}_{22}\overline{E}_{22}^{*})^{\dagger}\overline{E}_{21}.$$

Therefore, we get

$$\overline{X} = \begin{bmatrix} \Sigma_2^{-1} W \Sigma_3^{-1} & 0 \\ 0 & 0 \end{bmatrix}$$

from the relation

$$\begin{aligned} \begin{bmatrix} \Sigma_2 & 0 \end{bmatrix} \overline{X} \begin{bmatrix} \Sigma_3 \\ 0 \end{bmatrix} &= Z_{min} - \overline{E}_{11} \\ &= -\overline{E}_{11} - \overline{E}_{12}\overline{E}_{22}^{*}(\alpha^2 I - \overline{E}_{22}\overline{E}_{22}^{*})^{\dagger}\overline{E}_{21} \\ &=: W \end{aligned}$$

Hence the result. □

3.4.1 Summary of Design Procedure

We summarize the controller design procedure [13]. Given a minimal realization of a continuous-time system G, period T of periodic inputs to be tracked or rejected, the sampling period h in which the ratio $M := T/h$ is an integer, and the number of intersample points N. The design algorithm is:

Step 1: Starting with the minimal realization of G and obtain a realization of Φ_L (Appendix B).

Step 2: Parametrize all stabilizing controllers and get the matrices $\hat{\phi}_{11}$, $\hat{\phi}_{12}$ and $\hat{\phi}_{21}$.

Step 3: Find the solutions of $r(k)$ by the Lemma 3.4.2 that solve the M minimization problems:

$$\min_{r(k)} \overline{\sigma}[\hat{\phi}_{11}(\lambda_k) + \hat{\phi}_{12}(\lambda_k) r(\lambda_k) \hat{\phi}_{21}(\lambda_k)], \quad k = 0, ..., M-1.$$

The maximum of these minima is the optimal induced power of the system in Figure 3.4.

Step 4: Take the one-Mth of the inverse discrete Fourier transform of $r(k)$ to get $\tilde{r}(n)$. A minimizing $\hat{Q}(\lambda)$ is given by

$$\hat{Q}(\lambda) = \sum_{n=0}^{M-1} \tilde{r}(n)\lambda^n.$$

Step 5: Insert Q to arrive an optimal discrete-time controller $K_d = \mathcal{F}_l(J, Q)$.

The sampled-data optimal repetitive control problem 3.1

$$\min_{stabilizing\ K_d} ||\mathcal{F}_l(\Phi, K_d)||_{\Omega_{MN}}$$

is completely solved. Practical implementations of sampled-data repetitive control to CD player can be performed by the help of dSPACE.

Chapter 4

Preliminary Investigations and Proposal

4.1 Introduction

We have seen the theory of sampled-data repetitive control in the previous chapter. It turns out that, in order to track and/or reject signals, we only need to minimize the induced power of the system at certain frequencies (finitely many) on the unit circle in the λ-domain. Partial results can be obtained for continuous-time controller design via the decomposition of the continuous-time input signals into their Fourier components. A brief proposal will be given as a possible direction of sequential work.

4.2 Some Achievements

A discussion of Sampled-Data Digital Control was given in the last chapter. The author tried the possibility of discovering similar results in continuous-time repetitive control. The key step is to express a given periodic function (of period T) into its Fourier series and treat individual sinusoids independently. The output of the periodic function will naturally be the linear combination of the individual outputs. Of course, careful arguments on convergences should be considered. Some achievements will be presented in this section.

4.2.1 Mathematical Details

For the sake of completeness, we firstly give the definition of Laplace transform [7].

Definition 4.2.1 (Folland [7]). *Suppose $f : [0, \infty) \longrightarrow \mathbb{R}^p$ is piecewise continuous and satisfies an estimate*

$$|f(t)| \leq Ce^{at}$$

for some $C \geq 0$, $a \in \mathbb{R}$. The Laplace transform of f is defined as

$$(\mathscr{L}f)(s) := \int_0^\infty f(t)e^{-st}\, dt.$$

Note that the integral converges absolutely for $Re\ z > a$, and the convergence is uniform in the half-plane $Re\ z \geq a + \epsilon$ for any $\epsilon > 0$. Denote by $\mathcal{E}$ the class of all piecewise continuous functions in $\mathcal{L}(\mathbb{R}_+, \mathbb{R}^p)$ so that the bounded stated in Definition 4.2.1 is satisfied. The following theorem gives a fundamental result on continuous-time periodic functions.

Theorem 4.2.2. *Let $u : [0, \infty) \longrightarrow \mathbb{R}^p$ be periodic of period T and be such that its Laplace transform is well-defined (that is, $u \in \mathcal{W}_T \cap \mathcal{E}$). Then*

$$(\mathscr{L}u)(s) = \frac{1}{1 - e^{-sT}}\, U_0(s)$$

for some entire function $U_0(s)$.

Proof. Define

$$u_0(t) := \begin{cases} u(t), & t \in [0, T) \\ 0, & t > T \end{cases}$$

and define $U_0(s) := (\mathscr{L}u_0)(s)$. Then, result follows immediately. The analyticity of $U_0(s)$ can be verified by the validity of swapping the limit and the integral of the difference quotient using Dominated Convergence Theorem. □

From now on to the end of this chapter, we will concentrate on the class of periodic functions in which those functions can be expressed as their Fourier series and also Laplace transform is applicable. For the sake of simplicity, we consider those functions which are also continuous. Define

$$\mathcal{N}_T := \left\{ f \in \mathcal{W}_T \cap \mathcal{E} : f \text{ is piecewise } C^1 \text{ on } \mathbb{R}_+ \text{ and continuous on } \mathbb{R}_+ \right\}.$$

We know from Theorem 4.2.2 that the Laplace transform of a periodic function has a factor $1 - e^{-sT}$ in the demoninator. So, we are going to decompose this factor as an infinite sum of the principal parts so that analysis of individual harmonics is possible.

Definition 4.2.3 (Silverman [18]). *A function is called meromorphic if it is a quotient of two entire functions in which the denominator is not identically zero.*

Lemma 4.2.4 (Cauchy's Theorem on Partial Fraction Expansions). *Let $f(s)$ be a mermorphic function, and let $\{L_n\}$ be a sequence of closed rectifiable Jordan curves with the following properties:*

1. The origin lies inside each curve L_n $(n = 1, 2, ...)$;

2. None of the curves passes through poles of $f(s)$;

3. Each curve in the sequence is contained in the next, i.e. $L_n \subset I(L_{n+1})$;

4. If r_n is the distance from the origin to L_n, then

$$\lim_{n\to\infty} r_n = \infty.$$

Let the poles of $f(s)$ be ordered in such a way that L_n contains the first $m_n + 1$ poles $b_0 = 0, b_1, b_2, ..., b_{m_n}$, with principal parts $G_0(s)$, $G_1(s)$, ..., $G_{m_n}(s)$, so that $m_n \leq m_{n+1}$ $(n = 1, 2, ...)$. Moreover, suppose that

$$\overline{\lim_{n\to\infty}} \int_{L_n} \frac{|f(z)|}{|z|} ds = M < \infty \tag{4.1}$$

where $ds = |dz|$, and let s be an arbitary regular point of $f(s)$. Then

$$f(s) = \lim_{n\to\infty} \sum_{k=0}^{m_n} \left[G_k(s) + A_k\right],$$

where the constants A_k are given by the formula

$$A_k = Res_{z=b_k} \frac{f(z)}{z}$$

and the convergence of the series is uniformly on every compact set containing no poles of $f(s)$.

Proof. A special case of Theorem 14.11 in Silverman [18]. □

Remark 4.2.1. The bound condition 4.1 can be replaced by the following condition: suppose the sequence $\{L_n\}$ also has the property that there exists a constant $c > 0$ such that

$$\frac{l_n}{r_n} \leq c \quad (n = 1, 2, ...)$$

where l_n is the length of L_n, and the following bound

$$\overline{\lim_{n\to\infty}} \max_{z\in L_n} |f(z)| < \infty.$$

is satisfied.

Corollary 4.2.5. *The series*

$$\frac{1}{1-e^{-sT}} = \frac{1}{2} + \frac{1}{T}\left[\frac{1}{s} + \sum_{k=1}^{\infty}\left(\frac{1}{s-j\frac{2\pi}{T}k} + \frac{1}{s+j\frac{2\pi}{T}k}\right)\right]$$

holds for every point in the complex plane except the poles $j\frac{2\pi}{T}k$, $k \in \mathbb{Z}$. The series also converges uniformly on every compact set not containing the poles $j\frac{2\pi}{T}k$, $k \in \mathbb{Z}$.

Proof. Notice that the poles of

$$f(s) := \frac{1}{1-e^{-sT}}$$

are $j\frac{2\pi}{T}k$, $k \in \mathbb{Z}$ and they are all simple. The residues of the poles at $j\frac{2\pi}{T}k$, $k \in \mathbb{Z}$ are equal to $\frac{1}{T}$. We take the contours to be the squares with four corners at

$$\left(\pm\left[\frac{1}{2}+k\right]\frac{2\pi}{T}, \pm\left[\frac{1}{2}+k\right]\frac{2\pi}{T}\right)$$

where $k \in \mathbb{Z}_+$. That is,

$$L_k := \begin{cases} \left(\frac{1}{2}+k\right)\frac{2\pi}{T} + jy, & y \in \left[-\left(\frac{1}{2}+k\right)\frac{2\pi}{T}, \left(\frac{1}{2}+k\right)\frac{2\pi}{T}\right], \\ -x + j\left(\frac{1}{2}+k\right)\frac{2\pi}{T}, & x \in \left[-\left(\frac{1}{2}+k\right)\frac{2\pi}{T}, \left(\frac{1}{2}+k\right)\frac{2\pi}{T}\right], \\ -\left(\frac{1}{2}+k\right)\frac{2\pi}{T} - jy, & y \in \left[-\left(\frac{1}{2}+k\right)\frac{2\pi}{T}, \left(\frac{1}{2}+k\right)\frac{2\pi}{T}\right], \\ x - j\left(\frac{1}{2}+k\right)\frac{2\pi}{T}, & x \in \left[-\left(\frac{1}{2}+k\right)\frac{2\pi}{T}, \left(\frac{1}{2}+k\right)\frac{2\pi}{T}\right]. \end{cases}$$

In view of Theorem 4.2.4 and its remark,

$$l_k = 8 \cdot \left(\frac{1}{2}+k\right)\frac{2\pi}{T}$$

whereas

$$r_k = \left(\frac{1}{2}+k\right)\frac{2\pi}{T}.$$

The maximum

$$\max_{z \in L_k} |f(z)|$$

can be found to be

$$\frac{1}{1-e^{-\left(\frac{1}{2}+k\right)2\pi}},$$

which is uniformly bounded by $\frac{1}{1-e^{-\pi}}$ for every $k \in \mathbb{Z}$. The constants A_k are given by

$$A_k = Res_{z=j\frac{2\pi}{T}}\frac{f(z)}{z} = \frac{1}{j2\pi k}$$

for $k = \pm 1, \pm 2, \ldots$ and

$$A_0 = Res_{z=0}\frac{f(z)}{z} = \frac{1}{2}.$$

Result follows immediately. $\square$

For every continuous-time input $u \in \mathcal{N}_T$, express it as its Fourier series

$$u(t) = \sum_{k=-\infty}^{\infty} a_k e^{j\frac{2\pi}{T}kt}$$

where

$$a_k = \frac{1}{T}\int_0^T u(t)e^{-j\frac{2\pi}{T}t}\,dt.$$

Suppose the signal u is fed into a *stable* FDLTI continuous-time system P, then the Laplace transform of the output is

$$\begin{aligned}
\hat{Y}(s) &= \hat{P}(s)\hat{U}(s) \\
&= \hat{P}(s)\frac{\hat{U}_0(s)}{1-e^{-sT}} \\
&= \frac{\hat{P}(s)\hat{U}_0(s)}{2} + \frac{1}{T}\left[\frac{\hat{P}(s)\hat{U}_0(s)}{s}\right. \\
&\quad \left. + \sum_{k=1}^{\infty}\left(\frac{1}{s-j\frac{2\pi}{T}k} + \frac{1}{s+j\frac{2\pi}{T}k}\right)\hat{P}(s)\hat{U}_0(s)\right] \\
&= \frac{\hat{P}(s)\hat{U}_0(s)}{2} + \frac{1}{T}\left\{\frac{\hat{P}(s)-\hat{P}(0)}{s}\hat{U}_0(s)\right. \\
&\quad \left. + \sum_{k=1}^{\infty}\left(\frac{\hat{P}(s)-\hat{P}(j\frac{2\pi}{T}k)}{s-j\frac{2\pi}{T}k} + \frac{\hat{P}(s)-\hat{P}(-j\frac{2\pi}{T}k)}{s+j\frac{2\pi}{T}k}\right)\hat{U}_0(s)\right\} \\
&\quad + \frac{1}{T}\left\{\frac{\hat{P}(0)\hat{U}_0(s)}{s} + \sum_{k=1}^{\infty}\left(\frac{\hat{P}(j\frac{2\pi}{T}k)}{s-j\frac{2\pi}{T}k} + \frac{\hat{P}(-j\frac{2\pi}{T}k)}{s+j\frac{2\pi}{T}k}\right)\hat{U}_0(s)\right\}.
\end{aligned}$$

Denote

$$\begin{aligned}
\hat{Y}_{tr}(s) &:= \frac{\hat{P}(s)\hat{U}_0(s)}{2} + \frac{1}{T}\left\{\frac{\hat{P}(s)-\hat{P}(0)}{s}\hat{U}_0(s)\right. \\
&\quad \left. + \sum_{k=1}^{\infty}\left(\frac{\hat{P}(s)-\hat{P}(j\frac{2\pi}{T}k)}{s-j\frac{2\pi}{T}k} + \frac{\hat{P}(s)-\hat{P}(-j\frac{2\pi}{T}k)}{s+j\frac{2\pi}{T}k}\right)\hat{U}_0(s)\right\}
\end{aligned}$$

and

$$\hat{Y}_{ss}(s) := \frac{1}{T}\left\{\frac{\hat{P}(0)\hat{U}_0(s)}{s} + \sum_{k=1}^{\infty}\left(\frac{\hat{P}(j\frac{2\pi}{T}k)}{s-j\frac{2\pi}{T}k} + \frac{\hat{P}(-j\frac{2\pi}{T}k)}{s+j\frac{2\pi}{T}k}\right)\hat{U}_0(s)\right\}.$$

Suppose the stable plant P can be written as

$$\hat{P}(s) = \left[\begin{array}{c|c} A & B \\ \hline C & D \end{array}\right].$$

The series in $\hat{Y}_{tr}(s)$ converges absolutely and uniformly for any set not containing the eigenvalues of A. It is easy to verify the following relation:

$$\frac{\hat{P}(s_1) - \hat{P}(s_2)}{s_1 - s_2} = -C(s_1 I - A)^{-1}(s_2 I - A)^{-1}B$$

for every $s_1 \neq s_2 \in \mathbb{C}$. Recall that $\lambda_k = e^{j\frac{2\pi}{T}k}$, $k \in \mathbb{Z}_+$. So, the series in $\hat{Y}_{tr}(s)$ can be rewritten as

$$\begin{aligned} \hat{Y}_{tr}(s) &= \frac{\hat{P}(s)\hat{U}_0(s)}{2} \\ &\quad -\frac{1}{T}C(sI-A)^{-1}\left\{A^{-1} + \sum_{k=1}^{\infty}\left[(\lambda_k - A)^{-1} + (\overline{\lambda_k}I - A)^{-1}\right]\right\}B. \end{aligned}$$

Lemma 4.2.6. *The series*

$$\sum_{k=1}^{\infty}\left[(\lambda_k - A)^{-1} + (\overline{\lambda_k}I - A)^{-1}\right]$$

converges absolutely.

Proof. Denote by $||\cdot||$ a matrix norm. For large k, we have $||\frac{A}{\lambda_k}|| < 1$. Note also that

$$(\lambda_k - A)^{-1} + (\overline{\lambda_k}I - A)^{-1} = \frac{1}{\lambda_k}\left\{\left(I - \frac{A}{\lambda_k}\right)^{-1} - \left(I + \frac{A}{\lambda_k}\right)^{-1}\right\}.$$

Therefore, by expanding exponential of a matrix as a series, we obtain

$$(\lambda_k - A)^{-1} + (\overline{\lambda_k}I - A)^{-1} = \frac{2}{\lambda_k^2}A\left(I - \frac{A^2}{\lambda_k^2}\right)^{-1}.$$

Finally, for large k,

$$\begin{aligned} ||(\lambda_k - A)^{-1} + (\overline{\lambda_k}I - A)^{-1}|| &\leq \frac{2}{|\lambda_k|^2}||A|| \cdot \left\|\left(I - \frac{A^2}{\lambda_k^2}\right)^{-1}\right\| \\ &\leq 2 \cdot \frac{T^2}{4\pi k^2} \cdot ||A|| \cdot \frac{1}{1 - ||\frac{A^2}{\lambda_k^2}||} \\ &\leq c \cdot \frac{1}{k^2} \end{aligned}$$

for some constant c independent of k. $\square$

As an aftermath of Theorem 4.2.2, Lemma 4.2.6 and the previous discussions, we know by Final Value Theorem that the term $\hat{Y}_{tr}(s)$ is the transient state, that is, $y_{tr}(t)$ tends to zero as t tends to infinity. On the other hand, the inverse Laplace transform of each individual term in $\hat{Y}_{ss}(s)$ will tend to a sinusoid. In fact, for each $k \in \mathbb{Z}$,

$$\begin{aligned} \mathscr{L}^{-1}\left(\frac{\hat{U}_0(s)}{s - j\frac{2\pi}{T}k}\right) &= u_0(t) * \mathscr{L}^{-1}\left(\frac{1}{s - j\frac{2\pi}{T}k}\right)(t) \\ &= T a_k e^{j\frac{2\pi}{T}kt}, \quad t \geq 0, \end{aligned}$$

where the a_k's are Fourier coefficients of $u_0(t)$. This result can also be viewed from lifting technique stated in [2]. The input would then be a sequence in which each individual term is in a certain Banach space. For a periodic continuous-time input of period T, each individual term of the input sequence would be the same. The author arrives at the same result when putting the sequence $(e^{j\frac{2\pi}{T}kt}, e^{j\frac{2\pi}{T}kt}, \ldots)$ as the input in the lifted system.

Similar to the discussions in Chapter 2, we may mimic Theorem 3.3.3 to calculate the induced power of a continuous-time system over $\mathcal{W}_T$. We expect a similar form expression but the supremum is taking over all harmonic frequencies $j\frac{2\pi}{T}k$, $k \in \mathbb{Z}_+$. We also expect similar formulation of the repetitive control problem as a standard optimal control problem similar to problem 3.3. Further work has to be done. Careful convergence arguments are expected to be overcome.

4.3 Brief Proposal

In general term, the aim of this research is to study practical and theoretical aspects of control in the presence of periodic disturbances. In the medium term (six months to one year), it is expected to spend on equal effort on (i) practical work on CD player rig; and (ii) theoretical investigation. The former would require further familiarization with the experimental set-up and dSPACE. The latter would require reading and research in the areas of repetitive, adaptive and sampled-data control. A few, but not exhaustive, specific suggestions will be given in this section.

For the practical set-up, we have to design implementation schemes on the adaptive control of the sampled-data digital control (due to the variation of rotation speed of the disc). Another possibility of further research is the adoption of continuous-time controller and the comparison of the accuracies in using two types of controllers.

For the theoretical side, it is believed to be fruitful in using lifting technique in continuous-time controller design. The author attempted to use power in measuring continuous-time signals. However, one drawback is that power is *not* a genuine norm. An attempt of norm definition will be similar to Langari's technical report [13]. However, a theorem similar to Proposition 3.3.2 in the last chapter has to be established as a foundation for further arguments. Moreover, we decompose the continuous-time input signals as its Fourier series. It is conjectured that the values of the system at countably-infinite frequencies (that is, the harmonic frequencies) are sufficient to determine the power of that continuous-time system. This conjecture is natural because the (periodic) input signals are combinations of sinusoids at the harmonic frequencies and the system is linear. Therefore, the induced power of a system over a subclass of periodic continuous-time input will be no greater than the usual $\mathcal{H}_\infty$ norm of a stable system. As a sequel of the conjecture, it would be worthwhile to design some schemes in computing the maximum singular values of the system at particular frequencies, rather than on the whole imaginary axis. On the other hand, it is also necessary to discuss the "continuity" of the system so that Fourier representation can be used as a fundamental tool for further developments. (Here we treat the system as a mathematical operator.) So, a sensible definition of norm in the space of all continuous-time input/output signals should be sought. Also, we have to ensure that many daily life continuous-time systems are "continuous". Furthermore, the period of periodic input signals is not exact. Corresponding theory has to be juggled appropriately.

Appendix A

Standards of the Philips CD930 Model

Main Parameters

– Playing time, single side, two channels	approx. 60 min.
– Scanning velocity (2 channels)	$1.2 - 1.4 ms^{-1}$.
– Sense of rotation seen from the reading side	counterclockwise.
– Rotation speed of the disc	$3Hz$ (outermost track) to $8Hz$ (innermost track).
– Track pitch	$1.6 \pm 0.1\mu m$.
– Width of track	$0.4\mu m$.
– Pit depth	$0.1\mu m$.
– Diameter of the disc	$120mm$.
– Thickness of the disc	$1.2 \pm 0.1mm$.
– Diameter of centre hole	$15mm$.
– Starting diameter of program area	$50mm$.
– Refractive index of transparent substrate	1.55 ± 0.1.
– Number of channels	2 and/or 4 simultaneously sampled.
– Sampling frequency	$44.1kHz$.
– Quantization	16 bits linear/channel.
– Channel bit rate	$4.3218Mb/s$.

– Laser diode type	AlGaAs.
– Wavelength of laser	0.76 to $0.82\mu m$.
– Diameter of laser spot	$1\mu m$.
– Bandwidth of radial control loop	$500Hz$.
– Resonance frequency of the damping system in the radial control loop	$3,700Hz$.
– Bandwidth of focus control loop	$800Hz$.
– Resonance frequency of the damping system in the focus control loop	$40Hz$.

Typical Disturbances and Allowable Errors

– Radial eccentricity	$\pm 0.2mm$.
– Maximum deflection and up-and-down movement	$\pm 0.5mm$.
– Allowable radial error	$\pm 0.1\mu m$.
– Allowable focus error	$\pm 2\mu m$.

Appendix B

State-Space Representation of Φ_L

This appendix presents a state-space representation for Φ_L (Relation 3.2) in the designing procedure given a minimal realization of G

$$\hat{G}(s) = \left[\begin{array}{c|cc} \overline{A} & \overline{B}_1 & \overline{B}_2 \\ \hline \overline{C}_1 & \overline{D}_{11} & \overline{D}_{12} \\ \overline{C}_2 & \overline{D}_{21} & \overline{D}_{22} \end{array}\right].$$

By the definition of Φ_L,

$$\Phi_L := \begin{bmatrix} L & 0 \\ 0 & I \end{bmatrix} \begin{bmatrix} S_f & 0 \\ 0 & S \end{bmatrix} G \begin{bmatrix} H_f & 0 \\ 0 & H \end{bmatrix} \begin{bmatrix} L^{-1} & 0 \\ 0 & I \end{bmatrix}.$$

Define the matrices

$$\begin{aligned}
\underline{A}_d &:= e^{h\overline{A}} \\
\underline{B}_{2d} &:= \int_0^h e^{\tau\overline{A}}\, d\tau \\
A_f &:= e^{\frac{h}{N}\overline{A}} \\
[B_{1f}, B_{2f}] &:= \int_0^{h/N} e^{\tau\overline{A}}\, d\tau\, [\overline{B}_1, \overline{B}_2] \\
\underline{B}_1 &:= \begin{bmatrix} A_f^{N-1}B_{1f} & A_f^{N-2}B_{1f} & \cdots & B_{1f} \end{bmatrix} \\
\underline{C}_1 &:= \begin{bmatrix} \overline{C}_1 \\ \overline{C}_1 A_f \\ \vdots \\ \overline{C}_1 A_f^{N-1} \end{bmatrix}
\end{aligned}$$

$$
\begin{aligned}
\underline{C}_2 &:= \overline{C}_2 \\
\underline{D}_{11} &:= \begin{bmatrix} \overline{D}_{11} & 0 & \cdots & 0 \\ \overline{C}_1 B_{1f} & \overline{D}_{11} & \cdots & 0 \\ \vdots & \vdots & & \vdots \\ \overline{C}_1 A_f^{N-2} B_{1f} & \overline{C}_1 A_f^{N-3} B_{1f} & \cdots & \overline{D}_{11} \end{bmatrix} \\
\underline{D}_{12} &:= \begin{bmatrix} \overline{D}_{12} \\ \overline{C}_1 B_{2f} + \overline{D}_{12} \\ \vdots \\ \overline{C}_1 A_f^{N-2} B_{2f} + \cdots + \overline{C}_1 B_{2f} + \overline{D}_{12} \end{bmatrix} \\
\underline{D}_{21} &:= \begin{bmatrix} \overline{D}_{21} & 0 & \cdots & 0 \end{bmatrix} \\
\underline{D}_{22} &:= \overline{D}_{22}.
\end{aligned}
$$

The state-space representation of Φ_L is

$$
\begin{aligned}
\hat{\Phi}_L(\lambda) &:= \left[\begin{array}{c|cc} A & B_1 & B_2 \\ \hline C_1 & D_{11} & D_{12} \\ C_2 & D_{21} & D_{22} \end{array}\right] \\
&= \left[\begin{array}{c|cc} \underline{A}_d & \underline{B}_1 & \underline{B}_{2d} \\ \hline \underline{C}_1 & \underline{D}_{11} & \underline{D}_{12} \\ \underline{C}_2 & \underline{D}_{21} & \underline{D}_{22} \end{array}\right].
\end{aligned}
$$

Bibliography

[1] B. Bamieh, J.B. Pearson, B.A. Francis and A. Tannenbaum, A Lifting Technique for Linear Periodic Systems with Applications to Sampled-Data Control, *Systems and Control Letters*, **17**, (1991), 79-88.

[2] B.A. Bamieh and J.B. Pearson, A General Framework for Linear Periodic Systems with Applications to $\mathcal{H}^\infty$ Sampled-Data Control, *IEEE Transactions on Automatic Control*, **37**, (1992), 418-435.

[3] G. Bouwhuis, J. Braat, A. Huijser, J. Pasman, G. van Rosmalen and K. Schouhamer Immink, *Principles of Optical Disc Systems*, (1985), Adam Hilger Ltd., Bristol, UK.

[4] T. Chen and B.A. Francis, $\mathcal{H}_\infty$-Optimal Sampled-Data Control: Computation and Design, *Proceedings of the American Control Conference*, (1994), 2767-2771.

[5] J.C. Doyle, B.A. Francis and A.R. Tannenbaum, *Feedback Control Theory*, (1992), Macmillan Publishing Company, New York, USA.

[6] W. Draijer, Adaptive Control of the Philips Compact Disc Radial Servo System, *Technical Note Nr. 136/89*, Philips National Laboratory, (1989), 1-21.

[7] G.B. Folland, *Fourier Analysis and its Applications*, (1992), Wadsworth & Brooks/Cole Advanced Books & Software, Belmont, California, USA.

[8] B.A. Francis and W.M. Wonham, The Internal Model Principle of Control Theory, *Automatica*, **12**, (1976), 457-465.

[9] S. Hara and Y. Yamamoto, Stability of Repetitive Control Systems, *Proceedings of 24th Conference on Decision and Control*, (1985), 326-327.

[10] S. Hara, T. Omata and M. Nakano, Synthesis of Repetitive Control Systems and its Application, *Proceedings of 24th Conference on Decision and Control*, (1985), 1387-1392.

[11] S. Hara, Y. Yamamoto, T. Omata and M. Nakano, Repetitive Control System for Periodic Exogenous Signals, *IEEE Transactions on Automatic Control*, **33**, (1988), 659-668.

[12] J.P. Keller and B.D.O. Anderson, A New Approach to the Discretization of Continuous-Time Controllers, *IEEE Transactions on Automatic Control*, **37**, (1992), 214-223.

[13] A. Langari and B.A. Francis, Sampled-Data Repetitive Control Systems, *Technical Report*, Department of Electrical and Computer Engineering, University of Toronto, Canada, February 1994.

[14] A. Langari and B.A. Francis, Sampled-Data Repetitive Control Systems, *Proceedings of the American Control Conference*, (1994), 3234-3235.

[15] H. Nakajima and H. Ogawa, Translated by C. Aschmann, *Compact Disc Technology*, (1992), IOS Press, Oxford, England.

[16] A.V. Oppenheim and R.W. Schafer, *Discrete-Time Signal Processing*, (1989), Prentice-Hall, Inc., New Jersey, USA.

[17] F.R. Shaw and K. Srinivasan, Discrete-Time Repetitive Control System Design using the Regeneration Spectrum, *ASME Journal of Dynamic Systems, Measurement and Control*, **115**, (1993), 228-237.

[18] R.A. Silverman, *Introductory Somplex Analysis*, (1967), Prentice-Hall, Inc., New Jersey, USA.

[19] K. Srinivasan and C.L. Nachtigal, Analysis and Design of Machine Tool Chatter Control Systems Using the Regeneration Spectrum, *ASME Journal of Dynamic Systems, Measurement and Control*, **100**, (1978), 191-200.

[20] K. Srinivasan and F.R. Shaw, Analysis and Design of Repetitive Control Systems using the Regeneration Spectrum, *ASME Journal of Dynamic Systems, Measurement and Control*, **113**, (1991), 216-222.

[21] M. Tomizuka, T.C. Tsao and K.K. Chew, Discrete-Time Domain Analysis and Synthesis of Repetitive Controllers, *Proceedings of the American Control Conference*, (1988), 860-866.

[22] M. Tomizuka, T.C. Tsao and K.K. Chew, Analysis and Synthesis of Discrete-Time Repetitive Controllers, *ASME Journal of Dynamic Systems, Measurement and Control*, **111**, (1989), 353-358.

[23] M. Tomizuka, K.K. Chew and W.C. Yang, Disturbance Rejection through an External Model, *ASME Journal of Dynamic Systems, Measurement and Control*, **112**, (1990), 559-564.

[24] T.C. Tsao and M. Tomizuka, Adaptive and Repetitive Digital Control Algorithms for Noncircular Machining, *Proceedings of the American Control Conference*, (1988), 115-120.

[25] K. Zhou, J. Doyle and K. Glover, *Robust and Optimal Control* draft, (1993).